Theor Chem Acc (2002) 108:31–37
DOI 10.1007/s00214-002-0353-y

Theoretical
Chemistry Accounts

Regular article

Solvent effects on the electronic absorption spectrum of formamide studied by a sequential Monte Carlo/quantum mechanical approach

W. R. Rocha[1], **V. M. Martins**[1], **K. Coutinho**[2], **S. Canuto**[3]

[1] Núcleo de Estudos em Química Computacional, Departamento de Química, ICE, Universidade Federal de Juiz de Fora, UFJF, 36036-330 Juiz de Fora, MG, Brazil
[2] Universidade de Mogi das Cruzes/CCET, CP 411, 08701-970 Mogi das Cruzes, SP, Brazil
[3] Instituto de Física, Universidade de São Paulo, CP 66318, 05315-970 São Paulo, SP, Brazil

Received: 14 March 2002 / Accepted: 3 April 2002 / Published online: 24 June 2002

Abstract. Sequential Monte Carlo/quantum mechanical calculations are performed to study the solvent effects on the electronic absorption spectrum of formamide (FMA) in aqueous solution, varying from hydrogen bonds to the outer solvation shells. Full quantum-mechanical intermediate neglect of differential overlap/singly excited configuration interaction calculations are performed in the supermolecular structures generated by the Monte Carlo simulation. The largest calculation involves the ensemble average of 75 statistically uncorrelated quantum mechanical results obtained with the FMA solute surrounded by 150 water solvent molecules. We find that the $n \rightarrow \pi^*$ transition suffers a blueshift of 1,600 cm^{-1} upon solvation and the $\pi \rightarrow \pi^*$ transition undergoes a redshift of 800 cm^{-1}. On average, 1.5 hydrogen bonds are formed between FMA and water and these contribute with about 20% and about 30% of the total solvation shifts of the $n \rightarrow \pi^*$ and $\pi \rightarrow \pi^*$ transitions, respectively. The autocorrelation function of the energy is used to sample configurations from the Monte Carlo simulation, and the solvation shifts are shown to be converged values.

Key words: Formamide – QM/MM – Solvent effects – Absorption spectrum – Monte Carlo simulation

1 Introduction

The structural and spectroscopic changes of peptide groups (–CONH–) upon solvation have been of great interest for a long time. This interest is related to the fact that peptides are the main repetitive units of polypeptide chains and proteins. Therefore, understanding how these groups can interact with each other and with the surrounding solvent molecules can give insight into the complex intermolecular interactions that occur when proteins are solvated and also provide valuable information about the solvent effects on the structure and spectroscopic properties of these macromolecules.

With the aim of understanding the behavior of peptide groups in solution, several theoretical [1, 2, 3, 4, 5, 6, 7, 8, 9, 10] and experimental [11, 12, 13, 14] studies have been made on small peptide models such as *N*-methylacetamide, $CH_3CONHCH_3$, and formamide (FMA), $HCONH_2$. These works have focused mainly on the solvent effects on structural and vibrational properties; however, the study of the solvent effects on the electronic absorption spectra of peptide groups is sparse. The peptide group is the main chromophore of proteins, which has a weak $n \rightarrow \pi^*$ transition at about 220 nm (about 45,000 cm^{-1}) and a strong $\pi \rightarrow \pi^*$ transition at about 195 nm (about 51,000 cm^{-1}). The electronic transitions of most side chains occur below 200 nm and are masked by the intense $\pi \rightarrow \pi^*$ transition of the peptide groups [15]. As a result, the electronic absorption spectra of proteins in solution will resemble those of small peptide models in solution. For instance, it has been shown that the electronic spectra of random-coil and β-strand proteins have spectra very similar to peptide models such as *N*,*N*-dimethylacetamide [15], with the $\pi \rightarrow \pi^*$ absorption being redshifted. Time-resolved far-UV circular dichroism (CD) is today a powerful tool to monitor the pattern of the secondary structures of proteins [16]. The study of the normal electronic absorption spectrum of small peptide models plays an important role in obtaining good parameters for understanding the far-UV CD spectra of proteins [6, 7, 8, 9, 10, 17, 18].

The electronic spectrum of FMA in a vacuum is well understood [19] and comprises two Rydberg transitions, a weak $n \rightarrow \pi^*$ transition, an intense transition from the nonbonding π_{nb} orbital $\rightarrow \pi^*$ and a Q band, associated with the bonding π orbital $\rightarrow \pi^*$. However, the electronic spectrum of FMA in the condensed phase has not been studied extensively experimentally. From the theoretical point of view, the electronic spectrum of FMA has been studied in the gas phase [20, 21, 22, 23],

Correspondence to: S. Canuto
e-mail: canuto@if.usp.br

in clusters with up to three explicitly included water molecules [9, 24, 25, 26] and clusters inside a cavity [9]. In an early study, Del Bene [24], observed a blueshift in the $n \rightarrow \pi^*$ transition of FMA when complexed with one and two hydrogen-bonded water molecules. The magnitude of the blueshift was correlated with the strength of the hydrogen bond, which is weaker in the excited state. Sobolewski [25] has studied electronic transitions of FMA, involving the valence states, and performed calculations with FMA and one hydrogen-bonded water molecule, using the CASSCF/CASPT2 method. He found a transition energy of 48,635 cm^{-1} (0.01) for the $n \rightarrow \pi^*$ transition and 60,653 cm^{-1} (0.34) for the $\pi \rightarrow \pi^*$ transition of FMA. The $n \rightarrow \pi^*$ transition was blueshifted by 1,452 cm^{-1}, while the $\pi \rightarrow \pi^*$ transition was redshifted by 1,210 cm^{-1} relative to the gas phase, due only to the hydrogen bond with water. Besley and Hirst [7] have investigated the electronic spectrum of FMA in water, performing CASSCF/CASPT2 calculations within a self-consistent reaction field, with a repulsive potential to account for the Pauli repulsion between the solute and solvent. They found good agreement with the available experimental data, for the transitions involving valence and Rydberg states. These same authors have reported, more recently, the electronic spectrum of FMA in solution, using FMA–$(H_2O)_n$ ($n = 1$–3) complexes within a continuum dielectric [9]. They found that the presence of explicit water molecules destabilizes the Rydberg states of FMA by approximately 4,000 cm^{-1}. The valence $\pi \rightarrow \pi^*$ transition suffers a redshift of 2,016 cm^{-1} relative to the gas phase, with an increase of about 10% in its oscillator strength. The $n \rightarrow \pi^*$ transition undergoes a blueshift of 2,904 cm^{-1} for the FMA–$(H_2O)_1$ complex, increasing as the number of water molecules increases. The results reported so far for the solvatochromic shift of the $n \rightarrow \pi^*$ transition of FMA in water lies within the range 1,452–3,549 cm^{-1} for one [25] and three [26] hydrogen-bonded water molecules. There is a common sense between these previous works that to model the solvatochromic shift of the $n \rightarrow \pi^*$ transition of FMA in water, it may be necessary to consider more explicitly defined solvent molecules and many solvent configurations. In fact, it is clear that optimized hydrogen-bonded clusters do not represent the real situation in a liquid. Further, in a liquid all properties are configurational averages and the system is characterized by a large number of structures at a certain temperature.

In the present work we address to the electronic spectrum of FMA in aqueous solution, using a sequential Monte Carlo/quantum mechanical (S-MC/QM) procedure [27, 28, 29]. We perform a systematic study of the solvent effects on the valence $n \rightarrow \pi^*$ and $\pi \rightarrow \pi^*$ electronic transitions of FMA, where the solvent molecules are explicitly included in the QM calculations. In this approach we use MC simulations to generate structures of the liquid and subsequently perform QM calculations on those supermolecular structures, with all-valence electrons, to obtain the separate contributions of the different solvation shells to the specific electronic transition. The number of necessary solvation shells to be included can be analyzed systematically and converged results obtained [28]. As the number of configurations generated by the MC simulation is very high, the number of configurations to be submitted to subsequent QM calculations can be drastically reduced considering the statistical correlation between successive configurations generated by the MC simulations [27, 28, 30, 31]. In doing so, we are able to analyze the solvent effects varying from specific hydrogen-bond interactions up to the bulk limit. The largest calculation involves the ensemble average of 75 QM calculations performed on statistically uncorrelated structures obtained with the FMA solute surrounded by as many as 150 water solvent molecules. As presented later, the calculated values given for the solvatochromic shifts are statistically converged values. They are also converged with respect to the number of molecules included in each supermolecule. At the present stage, these large supermolecular QM calculations can only be made using semiempirical methods. The QM calculations start with a self-consistent-field intermediate neglect of differential overlap (INDO) calculation with a properly antisymmetric wavefunction with all valence electrons. The transition energies are obtained next using singly excited configuration interaction (CIS). As the number of solvent molecules explicitly included in the QM calculations is changed, the use of an extensive theory, such as CIS, is recommended. The S-MC/QM procedure differs from the conventional QM/MM method [32, 33, 34] in that all molecules –solute and solvent–are treated by quantum mechanics. The classical MC part is used only to generate the statistical structure of the liquid. Another important point is that all statistical information is obtained before running into the QM stage. This procedure has been successfully applied to study the solvent effects on the electronic spectrum of several systems, such as benzene [28] and β-carotene [29] in several different solvents, formaldehyde in water [35, 36], pyrimidine in water and in CCl_4 [37], acetone in water [38] and *N*-methylacetamide in water [39].

2 Theoretical methodology

MC statistical mechanics simulations were carried out employing standard procedures [40], including the Metropolis sampling technique and periodic boundary conditions using the minimum image method in a cubic box. The simulations were performed in the canonical (NVT) ensemble. The system consisted of one FMA molecule plus 400 solvent molecules (water). The volume of the cubic box was determined by the experimental density of water, which at 298.15 K is 0.9966 gcm^{-3}. The intermolecular interactions are described by the standard Lennard-Jones plus Coulomb potential with three parameters for each atom i (ε_i, σ_i and q_i). For the water molecules we used the simple point charge potential developed by van Gunsteren et al. [41]. For FMA, we used the optimized potential for liquid simulations potential [42], with the charges computed using the CHELPG fitting procedure [43], at the MP2/cc-pVDZ level of theory (Table 1). The intermolecular interactions were spherically truncated within a center-of-mass separation smaller than the cutoff radius, r_c, of 11.47 Å. Long-range corrections of the Lennard-Jones potential were calculated beyond this cutoff distance. In the simulation the molecules were kept with rigid geometries. The water molecules were kept in their C_{2v} structure with $r_{OH} = 1.000$ Å and $\angle HOH = 109.47°$. The FMA molecule was held rigid in its structure, optimized at the MP2/cc-pVDZ(d) level of theory, as shown in Fig. 1. The initial configurations were generated randomly, considering the position and orientation of each

Table 1. Intermolecular potential parameters used in the Monte Carlo simulations (q_i in elementary charge unit, ε_i in kilocalories per mole and σ_i in angstroms)

Molecule	Site	q_i	ε_i	σ_i
H_2O[a]	O	−0.820	0.155	3.165
	H	0.410	0.000	0.000
$HCNH_2$[b]	C	0.571	0.175	3.905
	N	−0.802	0.170	3.250
	O	−0.482	0.210	2.960
	H(CH)	−0.021	0.000	0.000
	H(NH)	0.367	0.000	0.000

[a] Simple point charge potential [41]
[b] Optimized potential for liquid simulation parameters [42] with the charges calculated using the CHELPG fitting procedure [43], at the MP2/cc-pVDZ level of theory

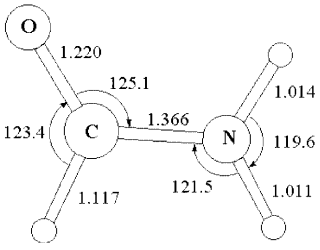

Fig. 1. MP2/cc-pVDZ optimized structural parameters for the formamide (*FMA*) molecule

molecule. The simulation consisted of a thermalization stage of 4×10^6 MC steps, followed by an averaging of 24×10^6 MC steps. To analyze the solvent effects on the electronic spectra of the FMA molecule we employed the S-MC/QM procedure [27, 28, 29], in which the QM calculations are performed on the supermolecular structures generated by the MC simulations. To analyze the convergence with the number of molecules included, the calculations were made with all solvent molecules within a particular solvation shell. Different solvation shells were considered. An important issue in all QM/MM methods is how to sample configurations from the statistical simulation. In our studies we sample configurations after analyzing the autocorrelation function of the energy [28, 30, 31, 35]. The use of the autocorrelation function of the energy for selecting configurations has been shown before to be an efficient procedure for obtaining converged average values [29, 30, 31]. In this present study we selected a total of 75 configurations, for each solvation shell, with less than 12% of statistical correlation. These configurations were used in the QM calculations. As we shall see later, the results obtained here are converged. The solvation shells were defined in the usual way, using the radial distribution function. The electronic spectra were then calculated using the semiempirical ZINDO [44] program, within the INDO/CIS [45] approach. As the appropriate Boltzmann weights are included in the Metropolis MC sampling technique, the average value of the transition energies and solvatochromic shifts are given as a simple average over the chain of calculated uncorrelated results.

All the ab initio calculations reported here were performed using the Gaussian98 program [46]. The MC statistical mechanics simulations were performed using the DICE program [47]. DICE is a general program for MC simulations that calculates thermodynamic properties and generates structures for use in most conventional quantum chemistry programs.

3 Results and discussion

3.1 Hydrogen bond

An important point in the solvation of FMA in water is the formation of hydrogen bonds. The radial pair distribution function between the carbonyl oxygen of FMA and the water hydrogen, $g_{O\text{-}H}(r)$, is shown in Fig. 2 and the radial pair distribution function between the amino hydrogen of FMA and the water oxygen, $g_{H\text{-}O}(r)$, is shown in Fig. 3. Hydrogen-bonded structures are conventionally obtained from the analysis of the radial distribution functions $g_{O\text{-}H}(r)$ and $g_{H\text{-}O}(r)$ and these are shown in Figs. 2 and 3. The first peak in the $g_{O\text{-}H}(r)$ distribution function starts at 1.45 Å, reaches its maximum at 1.85 Å and ends at 2.55 Å. For $g_{H\text{-}O}(r)$, the first peak starts at 1.55 Å, passes through a maximum at 1.95 Å and ends at 2.55 Å. The spherical integration of the first peak in $g_{O\text{-}H}(r)$ and $g_{H\text{-}O}(r)$ over the corresponding intervals gives 1.0 and 0.9 water molecules as nearest neighbors, respectively.

Hydrogen bonds in liquids are better obtained using geometric and energetic criteria, as discussed before by Stilinger and Rahman [48] and Mezei and Beveridge [49]. Indeed, these are more appropriate [48, 49, 50] to study solvent effects in spectroscopy [35]. We consider here a hydrogen-bond formation when the distance $R_{DA} \leq 4$ Å,

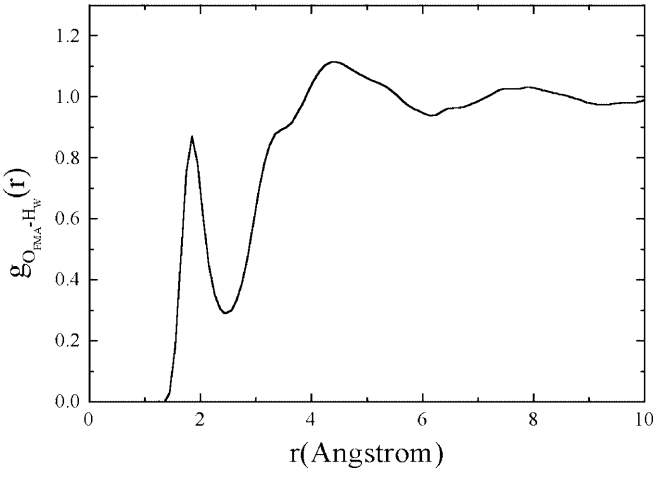

Fig. 2. Radial pair distribution function between the carbonyl oxygen of FMA and the hydrogen of water

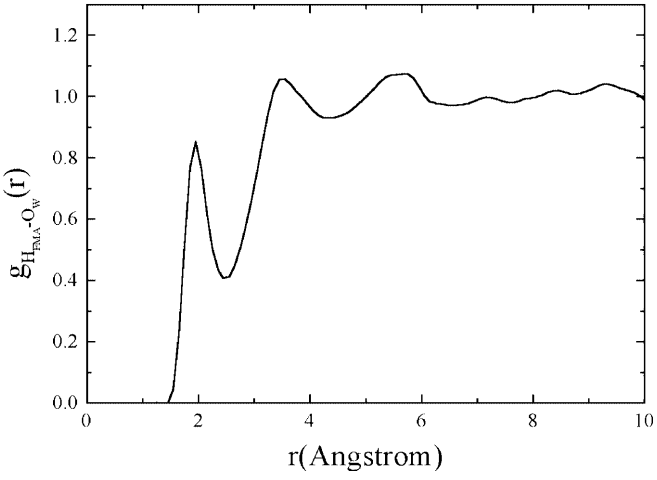

Fig. 3. Radial pair distribution function between the hydrogen atom of FMA (N–H) and the oxygen atom of water

the angle ∠AHD ≤ 30° and the binding energy is higher than 3.0 kcalmol^{-1}. In doing so, in the 75 MC configurations we find 109 hydrogen bonds formed between FMA and water molecules. This gives an average of 1.5 hydrogen bonds. Note that these are averages for the liquid. FMA can form up to three hydrogen bonds with the surrounding water molecules and the statistics obtained for the hydrogen bonds formed are given in Table 2. We find that in 12% of the configurations, FMA does not form hydrogen bonds, in 43% it forms one, in 33% it forms two and in 12% it forms three hydrogen bonds. The average classical values computed for the hydrogen binding energy when the carbonyl oxygen of FMA acts as a proton acceptor and when the NH group acts as a proton donor are 6.1 and 5.0 kcalmol^{-1}, respectively.

3.2 Electronic spectrum

The calculated solvatochromic shifts on the electronic transitions of FMA, due only to the hydrogen bonds between FMA and water, are also shown in Table 2. The $n \rightarrow \pi^*$ transition of FMA suffers a blueshift of 310 cm^{-1} due only to one hydrogen-bonding interaction. The blueshift increases as the number of hydrogen bonds increases, being 432 and 850 cm^{-1} due to two and three hydrogen bonds, respectively. Similar trends are observed for the $\pi \rightarrow \pi^*$ transition which undergoes a redshift of 116 cm^{-1} due to one hydrogen-bond interaction and increases to 385 and 1101 cm^{-1} due to two and three hydrogen bonds, respectively. On average, the hydrogen-bond shell contributes 379 ± 58 cm^{-1} to the blueshift of the $n \rightarrow \pi^*$ transition and 320 ± 96 cm^{-1} to the redshift of the $\pi \rightarrow \pi^*$ transition of FMA. Note that these hydrogen-bond contributions given in Table 2 are obtained using the structures obtained from the liquid. These structures give a solvation shift that is considerably smaller than that obtained using optimized clusters. Again, in the liquid the results, as reported here, are obtained using averages of different structures generated at room temperature. To analyze the effect on the number of molecules around the FMA molecule we use the radial distribution function, $g(r)$, of the center of masses. $g_{\text{cm-cm}}(r)$ calculated for the FMA molecule in water solution is depicted in Fig. 4, where two solvation shells are easily distinguished. The first solvation shell starts at 2.65 Å and extends up to 5.75 Å; the second solvation shell ends at 8.65 Å. Spherical integration of $g_{\text{cm-cm}}(r)$ over the corresponding intervals gives 25 and 96 water molecules in the first and second solvation shells, respectively. Since the liquid is not structured beyond the second solvation shell, to go beyond we used solvent molecules up to a maximum of 150 water molecules. This corresponds to all water molecules within a radius of 10.25 Å. For each shell 75 QM calculations of the electronic spectrum were performed and the values of the transition energies were averaged out. The results obtained are reported in Table 3. Our largest calculation, made for the outermost shell, includes one FMA molecule and 150 water molecules, with 1,218 valence electrons explicitly included. The corresponding calculated shifts for the $n \rightarrow \pi^*$ and $\pi \rightarrow \pi^*$ transitions of FMA in these largest structures are 1,558 ± 59 and −757 ± 65 cm^{-1}, respectively. The results in Table 3 show that the solvatochromic shifts are nearly converged with respect to the number of water molecules included in the supermolec-

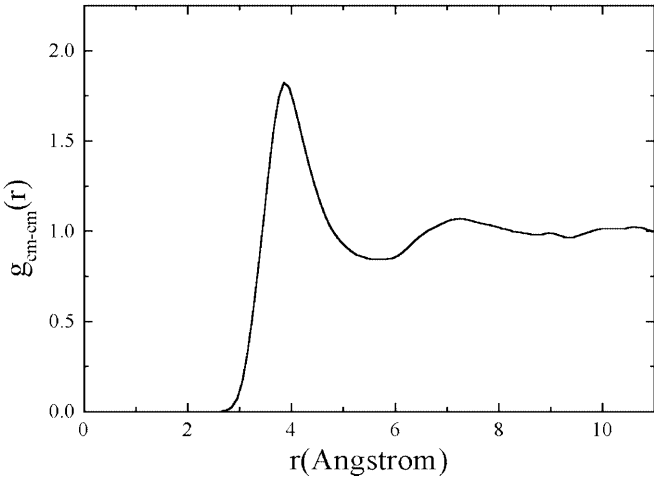

Fig. 4. Radial pair distribution function between the FMA center of mass and the water center of mass

Table 2. Statistics of the hydrogen bonds formed between formamide (*FMA*) and water and their contribution to the solvatochromic shifts of the $n \rightarrow \pi^*$ and $\pi \rightarrow \pi^*$ transitions. The absolute intermediate neglect of differential overlap (*INDO*)/singly excited configuration interaction (*CIS*) transition energies, computed in the gas phase, for the $n \rightarrow \pi^*$ and $\pi \rightarrow \pi^*$ transitions of FMA are 36,100 and 60,503 cm^{-1}, respectively, with oscillator strengths of 0.001 and 0.320, respectively

Number of hydrogen bonds	Occurrence (%)	$n \rightarrow \pi^*$ shift (cm^{-1})	$\pi \rightarrow \pi^*$ shift (cm^{-1})
0	12	–	–
1	43	310	−116
2	33	432	−385
3	12	850	−1,101
Total	100	379 ± 58	−320 ± 96

Table 3. Variation of the calculated (INDO/CIS) shifts of the $n \rightarrow \pi^*$ and $\pi \rightarrow \pi^*$ transitions of FMA in water with the solvation shells. *N* is the total number of water molecules included. *M* is the total number of valence electrons included in the quantum mechanical calculations. *r* is the distance of the radial distribution function. Each solvatochromic shift shown is the result of an average of 75 quantum mechanical calculations. See text

N	*M*	*r* (Å)	$n \rightarrow \pi^*$ shift (cm^{-1})	$\pi \rightarrow \pi^*$ shift (cm^{-1})
25	218	5.75	1,131 ± 54	−558 ± 72
55	458	7.45	1,347 ± 54	−692 ± 64
96	786	8.85	1,481 ± 57	−770 ± 68
120	978	9.55	1,529 ± 57	−781 ± 69
150	1,218	10.25	1,558 ± 59	−757 ± 65
Limit			1,600 ± 59	−800 ± 65

ular structures. The calculated solvatochromic shifts for the $n \rightarrow \pi^*$ and $\pi \rightarrow \pi^*$ transitions of FMA as a function of the number of water molecules included can be seen in Fig. 5. The monotonic behavior of the calculated energy shift for the $n \rightarrow \pi^*$ and $\pi \rightarrow \pi^*$ transitions of FMA permits the extrapolation of the results to the bulk limit. In doing so we obtain limiting values of 1,600 and $-800\ cm^{-1}$ for the $n \rightarrow \pi^*$ and $\pi \rightarrow \pi^*$ transitions. This would be our best estimate for the solvatochromic shifts of the $n \rightarrow \pi^*$ and $\pi \rightarrow \pi^*$ electronic transitions of FMA in aqueous solution. Unfortunately an experimental value is not available for comparison. These numbers are however in close agreement with those obtained in a similar study for *N*-methylacetamide [39].

The solvatochromic shift of the $n \rightarrow \pi^*$ transition, due only to the hydrogen-bond interactions, represents about 20% of the total shift extrapolated to the bulk limit. For the $\pi \rightarrow \pi^*$ transition, hydrogen bonds contributes to about 30% of the total shift. Our results obtained for the hydrogen-bond contribution to the solvent shifts of the $n \rightarrow \pi^*$ and $\pi \rightarrow \pi^*$ transitions of FMA in aqueous solution are lower when compared with previous results for FMA-$(H_2O)_n$ ($n = 1$–3) cluster calculations [9, 24, 25, 26]. However, it is important to realize that in the cluster the hydrogen-bond interaction is stronger than in the liquid, as in this case the water is also bound to other water molecules. Another aspect is that in the liquid several structures are possible at a given temperature and not only a minimum energy as in the case of the optimized cluster. As a result, the calculation using the optimized gas-phase structure overestimates the hydrogen bond and does not reproduce the situation of the liquid. This has been noted before for acetone in water [38].

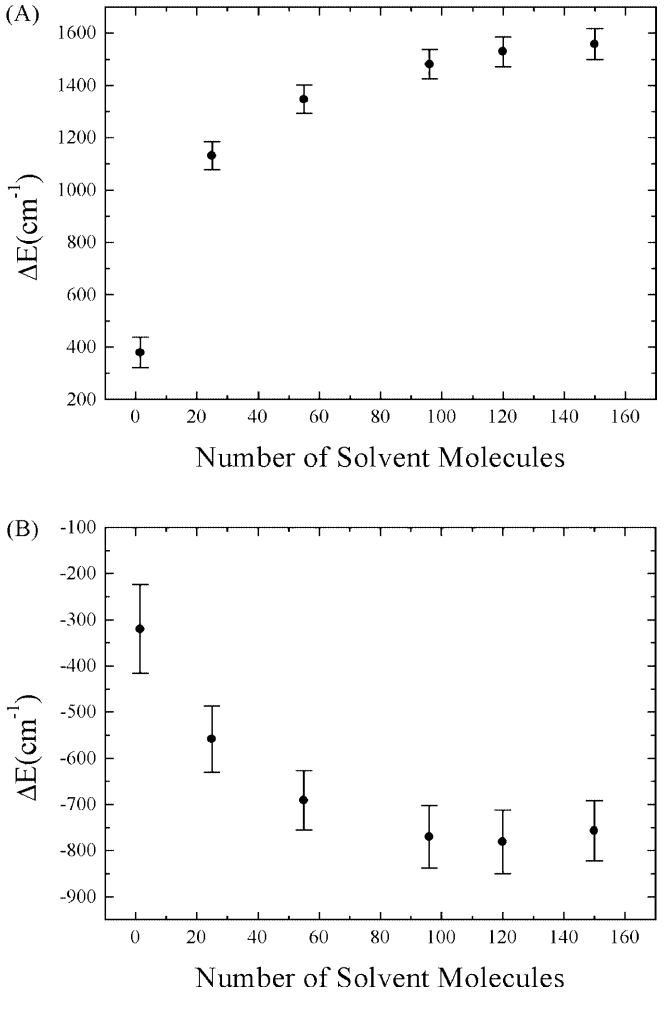

Fig. 5. Calculated solvatochromic shift for **A** the $n \rightarrow \pi^*$ and **B** the $\pi \rightarrow \pi^*$ transition of FMA in water, as a function of the number of solvent molecules

3.3 Sampling and statistical convergence

As the calculated average values obtained here are derived from several QM calculations using the structures of the simulation, it is important now to discuss the convergence of the final result. It is also convenient to show the statistical efficiency obtained with the autocorrelation function of the energy. In doing so, the subsequent QM calculations are performed only on some uncorrelated structures. This is one of the advantages of the S-MC/QM procedure, in that all the important MC statistical information is available before running into the QM calculations. As in previous work [28, 29, 30, 31, 35, 36, 37] we calculate the autocorrelation function of the energy, $C(n)$, to obtain the interval of statistical correlation, using the definition

$$C(n) = \frac{\langle \delta E_i E_{i+n} \rangle}{\langle \delta E^2 \rangle} = \frac{\sum_i (E_i - \langle E \rangle)(E_{i+n} - \langle E \rangle)}{\sum_i (E_i - \langle E \rangle)^2} \quad ,$$

where E_i is the energy of configuration i and E_{i+n} is the energy of the configuration generated n MC steps later. For Markovian processes, it is known that $C(n)$ follows an exponential decay [28, 35], $C(n) = \exp(-n/\tau)$, and represents the statistical correlation between configurations separated by n MC steps. In practice, the configurations are considered statistically uncorrelated for an interval $n \approx 2\tau$. For FMA in water, we find that configurations separated by 3.2×10^5 MC steps are 10% correlated. Using configurations separated by much less than this is a waste because the calculation includes configurations that do not contribute to the average. Thus, out of the simulation of 24×10^6 MC steps we use only 75 configurations. The dependence of our calculated solvation shift on the number of configurations used for the $n \rightarrow \pi^*$ transition is shown in Fig. 6. The results show the convergence of the average value. This is a demonstration of the efficiency of the use of the autocorrelation function in that only a few instantaneous values give statistically converged results. Thus, the use of the interval of the statistical correlation (2τ) obtained using the autocorrelation function of the energy is a very effective way to sample configurations giving statistically converged results with a relatively small number of calculations, because only statistically relevant configurations are included. Our present results

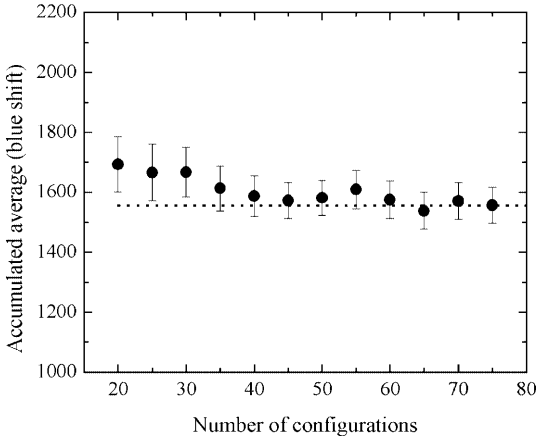

Fig. 6. Convergence of the calculated solvation shifts (cm^{-1}) of the $n \rightarrow \pi^*$ transition of FMA in water

are converged values incorporating the inherent statistical nature of the liquid.

4 Summary and conclusions

In this work we employed a S-MC/QM procedure to analyze the solvent effects on the $n \rightarrow \pi^*$ and $\pi \rightarrow \pi^*$ electronic transitions of FMA in aqueous solution. The structural analysis of the solution, by means of the radial pair distribution function, showed that FMA can form up to three hydrogen bonds with water. The hydrogen-bond statistics revealed that in 12% of the configurations FMA does not form any hydrogen bonds with water, but in 43% forms one, in 33% forms two and in 12% forms three hydrogen bonds. The $n \rightarrow \pi^*$ transition of FMA suffers a blueshift of $379 \pm 58\ cm^{-1}$ due only to hydrogen-bonding interactions. Similarly, the $\pi \rightarrow \pi^*$ transition undergoes a redshift of $320 \pm 96\ cm^{-1}$. Next, 75 QM calculations were made for each of the first, second and outer solvation shells. To verify convergence with the number of molecules included in the supermolecules, calculations were made including all water molecules up to the limit radius of 10.25 Å. We find that the $n \rightarrow \pi^*$ transition suffers a blueshift of 1,600 cm^{-1} upon solvation and the $\pi \rightarrow \pi^*$ transition undergoes a redshift of 800 cm^{-1}. Statistical convergence is obtained using the autocorrelation function of the energy to sample the configurations from the MC simulation. The solvation shifts reported here are thus converged values both with respect to the number of molecules explicitly included as well as the number of configurations used for the statistical averages. The sequential use of the MC and QM calculations allows the advantageous use of the statistical information before the QM calculations. Also, all molecules within a particular supermolecular structure are treated by quantum mechanics, thus including the important polarization effects.

Acknowledgements. This work was partially supported by CNPq and FAPESP (Brazil). V.M.M. thanks the BIC/UFJF for an undergraduate scholarship.

References

1. McCreery, Christoffersen RE, Hall GG (1976) J Am Chem Soc 98: 7198
2. Marchese FT, Mehrota PK, Beveridge DL (1984) J Phys Chem 88: 5692
3. Jorgensen WL, Swenson CJ (1985) J Am Chem Soc 107: 1489
4. Sim F, St-Amant A, Papai I, Salahub DR (1992) J Am Chem Soc 114: 4391
5. Contador JC, Sanchez ML, Aguilar ML, Olivares Del Valle FJ (1996) J Chem Phys 104: 5539
6. Hirst JD (1998) J Chem Phys 109: 782
7. Besley NA, Hirst JD (1998) J Phys Chem A 102: 10791
8. Woody RW, Sreerama N (1999) J Chem Phys 111: 2844
9. Besley NA, Hirst JD (1999) J Am Chem Soc 121: 8559
10. Besley NA, Hirst JD (2000) J Mol Struct (THEOCHEM) 506: 161
11. Kuznetsova LM, Furer VL, Maklakov LI (1996) J Mol Struct 380: 23
12. Sieler G, Schweitzer-Stenner R (1997) J Am Chem Soc 119: 1720
13. Ludwig R, Weinhold F, Farrar TC (1997) J Phys Chem A 101: 8861
14. Schweitzer-Stenner R, Sieler G, Mirkin NG, Krimm S (1998) J Phys Chem A 102: 118
15. Van Holde KE, Johnson WC, Ho PS (1998) Principles of physical biochemistry. Prentice-Hall, New Jersey
16. Woody RW (1995) Methods Enzymol 246: 34
17. Clark LB (1995) J Am Chem Soc 117: 7974
18. Woody RW, Raabe G, Fleischhauer J (1999) J Phys Chem A 103: 8984
19. Gingell JM, Mason NJ, Zhao H, Walker IC, Siggel MRS (1997) Chem Phys 220: 191
20. Hirst JD, Hirst DM, Brooks CL III (1996) J Phys Chem A 100: 13487
21. Serrano-Andrés L, Fülsher MP (1996) J Am Chem Soc 118: 12190
22. Hirst JD, Hirst DM, Brooks CL III (1997) J Phys Chem A 101: 4821
23. Szalay P, Foragasi G (1997) Chem Phys Lett 270: 406
24. Del Bene JE (1975) J Chem Phys 62: 1961
25. Sobolewski AL (1995) Photochem Photobiol 89: 89
26. Krauss M, Webb SP (1997) J Chem Phys 107: 5771
27. Coutinho K, Canuto S (1997) Adv Quantum Chem 28: 89
28. Coutinho K, Canuto S, Zerner MC (2000) J Chem Phys 112: 9874
29. Canuto S, Coutinho K, Trzesniak D (2002) Adv Quantum Chem (in press)
30. Coutinho K, De Oliveira MJ, Canuto S (1998) Int J Quantum Chem 66: 249
31. Rocha WR, Coutinho K, De Almeida WB, Canuto S (2001) Chem Phys Lett 335: 127
32. Warshel A, Levitt M (1976) J Mol Biol 103: 227
33. Field MJ, Basch PA, Karplus M (1990) J Comput Chem 11: 700
34. Gao J, Xia X (1992) Science 258: 631
35. Canuto S, Coutinho K (2000) Int J Quantum Chem 77: 192
36. Coutinho K, Canuto S (2000) J Chem Phys 113: 9132
37. De Almeida KJ, Coutinho K, De Almeida WB, Rocha WR, Canuto S (2001) Phys Chem Chem Phys 3: 1583
38. Coutinho K, Saavedra N, Canuto S (1999) J Mol Struct (THEOCHEM) 466: 69
39. Rocha WR, De Almeida KJ, Coutinho K, Canuto S (2001) Chem Phys Lett 345: 171
40. Allen MP, Tildesley DJ (1987) Computer simulation of liquids. Oxford University Press, Oxford
41. Berendsen HJC, Postma JPM, van Gunsteren WF (1981) In: Pullman B (ed) Intermolecular forces. Reidel, Dordrecht p 331
42. Damm W, Frontera A, Tirado-Rives J, Jorgensen WL (1997) J Comput Chem 18: 1995
43. Breneman CM, Wiberg KB (1990) J Comput Chem 11: 361
44. Zerner MC ZINDO: a semiempirical program package. University of Florida, Gainesville, Fla

45. Ridley J, Zerner MC (1973) Theor Chim Acta 32: 111
46. Frisch MJ, Trucks GW, Schlegel HB, Scuseria GE, Robb MA, Cheeseman JR, Zakrzewski VG, Montgomery JA Jr, Stratmann RE, Burant JC, Dapprich S, Millam JM, Daniels AD, Kudin KN, Strain MC, Farkas O, Tomasi J, Barone V, Cossi M, Cammi R, Mennucci B, Pomelli C, Adamo C, Clifford S, Ochterski J, Petersson GA, Ayala PY, Cui Q, Morokuma K, Malick DK, Rabuck AD, Raghavachari K, Foresman JB, Cioslowski J, Ortiz JV, Stefanov BB, Liu G, Liashenko A, Piskorz P, Komaromi I, Gomperts R, Martin RL, Fox DJ, Keith T, Al-Laham MA, Peng CY, Nanayakkara A, Gonzalez C, Challacombe M, Gill PMW, Johnson B, Chen W, Wong MW, Andres JL, Head-Gordon M, Replogle ES, Pople JA (1998) Gaussian 98, revision A.6. Gaussian, Pittsburgh, Pa
47. Coutinho K, Canuto S (1997) DICE: a Monte Carlo program for liquid simulation. University of São Paulo, São Paulo
48. Stilinger FH, Rahman A (1974) J Chem Phys 60: 3336
49. Mezei M, Beveridge DL (1981) J Chem Phys 74: 622
50. Jorgensen WL, Chandrasekhar J, Madura JD, Impey RW, Klein ML (1983) J Chem Phys 79: 926